

Energy and angular distributions in dissociative photodetachment of O_4^-

C. R. Sherwood, M. C. Garner, K. A. Hanold, K. M. Strong, and R. E. Continetti
*Department of Chemistry and Biochemistry, University of California, San Diego, 9500 Gilman Drive,
La Jolla, California 92093-0314*

(Received 20 January 1995; accepted 24 February 1995)

An anisotropic product angular distribution has been observed in the dissociative photodetachment of O_4^- at 523 nm. Energy and angular distributions of coincident O_2 products from the process $O_4^- + h\nu \rightarrow O_2 + O_2 + e^-$ were measured using translational energy spectroscopy in a fast ion beam. The angular distribution peaks perpendicular to the electric vector of the laser beam. © 1995 American Institute of Physics.

Analyses of product energy and angular distributions have provided important insights into the dynamics of both bimolecular and unimolecular chemical reactions. In the case of photodissociation, it has been shown^{1,2} that product angular distributions are affected by excited state lifetimes, molecular structure and electronic symmetry. Anisotropic product angular distributions have been observed in dissociative photoionization,³ dissociative electron-impact ionization,⁴ and dissociative electron attachment to neutral molecules.⁵ An anisotropic distribution of molecular axes is also expected to be produced in photodetachment of a negative ion, by analogy to the treatment of photoionization by Greene and Zare.⁶ In this letter, the first observation of an anisotropic molecular product angular distribution in dissociative photodetachment is reported. By measuring product kinetic energy and angular distributions, we have observed this effect in the photodestruction of the tetroxide anion, O_4^- , at 523 nm.

Dissociative photodetachment (DPD) occurs when the neutral complex left behind by electron photodetachment is unstable. Photoelectron spectroscopy has been used to study the dynamics of the photodetachment of molecular anions producing unstable neutral products.⁷ Little attention has previously been paid to the fate of the transient neutral species produced in these photodetachment experiments. The present experiment shows that in the case of O_4^- , photodetachment and dissociation occur promptly on the time scale of molecular rotation.

O_4^- is known to photodestruct in the 200 to 1000 nm range from total cross-section measurements.⁸ Gas-phase thermochemical measurements indicate that O_4^- is stable with respect to dissociation into $O_2 + O_2^-$ by 0.46 ± 0.02 eV.⁹ This is in accord with semi-empirical self-consistent-field calculations, which predicted that O_4^- is a planar species stable with respect to dissociation into $O_2 + O_2^-$ by ≈ 0.4 eV.¹⁰ More recent unrestricted Hartree-Fock *ab initio* calculations¹¹ have predicted a binding energy of only ≈ 0.1 eV, far below the experimental values. The relatively high observed binding energy suggests that the bonding in this homomolecular cluster anion may be strengthened by significant electron delocalization.¹²

The experiments described here make use of translational energy spectroscopy in a fast negative-ion beam. The design of the apparatus is similar to that used by Neumark and co-workers to study free-radical photodissociation.¹³ Anions are produced and cooled in a pulsed free-jet expansion

of O_2 intersecting a 1 keV electron beam.¹⁴ The anions pass through a skimmer into a differentially pumped chamber, are accelerated to kinetic energies of 2–7 keV, and mass selected by time of flight. Anions at the mass of interest are intersected by the linearly polarized frequency-doubled output of a Nd:YLF laser (Spectra Physics TFR). The laser pulse is 6 ns full-width-at-half-maximum with an energy of 200 μ J/pulse at 523 nm and is focused to a spot of ≈ 0.5 mm diameter at the interaction region. The apparatus runs at a repetition rate of 500 Hz.

Photofragments recoil out of the beam as it traverses a 95 cm flight path between the laser interaction region and a particle detector. Those that clear a 7 mm wide beam-block strip, centered on the ion beam, strike a 46 mm diam microchannel-plate particle detector. This detector makes use of two side-by-side wedge-and-strip anodes¹⁵ to record the time and position of arrival of fragments. The detector face is at ground potential, allowing both neutral and ionic products to be detected. Detector calibration was performed by recording data on the photodissociation of O_2^- at 262 nm,¹⁵ and showed that the energy resolution is ≈ 70 meV.

There are two possible modes of data acquisition—collection of neutral fragments *or* neutral and ionic fragments. Electrostatic deflection of ions out of the beam after the laser interaction region allows detection of only neutral products. If no deflection field is used, both ionic and neutral products are detected. The data presented consists only of the pairs of *coincident* fragments that originate from a single dissociation event. These fragments conserve momentum in the center-of-mass frame. Photofragment pairs that do not conserve momentum are discarded as false coincidences. Detection of the fragments in coincidence allows determination of the product masses, translational energy release and center-of-mass recoil angle for each dissociation event.^{13,16} Only equal-mass products (i.e., $O_2 + O_2$ or $O_2 + O_2^-$) were observed from the photodestruction of O_4^- at 523 nm.

Translational energy release spectra recorded with the laser polarized along the direction of the ion beam are shown in Fig. 1. The spectrum for coincident neutrals at full laser power (middle curve in Fig. 1) shows two main features—a peak near 0.8 eV and a much larger peak at 0.4 eV. Comparison with a coincidence spectrum that includes both neutral and ionic fragments (top curve in Fig. 1) shows that the higher energy peak is due to the photodissociation $O_4^- + h\nu \rightarrow O_2 + O_2^-$.^{17,18} The dynamics of this photodissocia-

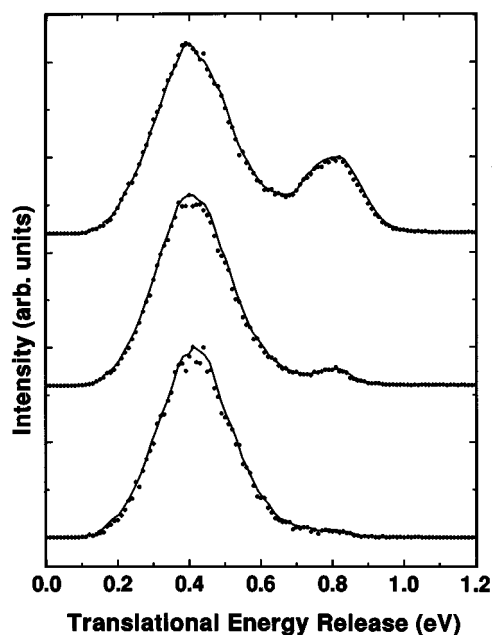


FIG. 1. Translational energy release distributions recorded for coincident O_2 and O_2^- photofragments with the electric vector of the laser oriented along the direction of the incident ion beam. The solid lines correspond to the center-of-mass translational energy distribution $P(E_T)$. The points correspond to raw experimental data. Top curve: coincident ions and neutrals, middle curve: coincident neutrals, bottom curve: coincident neutrals at reduced laser power.

tion will be discussed further in a forthcoming publication.¹⁹ Reduction of the laser power by a factor of 10 yields the bottom curve in Fig. 1. Comparison of the middle and bottom curves shows that the only power-dependent feature is the peak at 0.8 eV due to photodissociation. This power-dependent peak is seen in the neutral spectrum at full laser power due to photodetachment of nascent O_2^- by a second photon. The peak at 0.4 eV is assigned to DPD: $O_4^- + h\nu \rightarrow O_2 + O_2 + e^-$.

The data contain a three-dimensional record of the energy and angular distributions of the photofragments. The anisotropy of the angular distribution as a function of translational energy release (E_T) can be found by separating the doubly differential cross section $P(E_T, \theta)$ into energy and angle distributions as $P(E_T, \theta) = P(E_T)[1 + \beta(E_T)P_2(\cos \theta)]$.¹³ The angular dependence of this function at a given energy is given by the standard electric-dipole form $I(\theta) = 1 + \beta P_2(\cos \theta)$, where $P_2(\cos \theta)$ is the second Legendre polynomial in $\cos \theta$ and θ is the angle between the center-of-mass recoil velocity and the electric vector of the laser beam.^{1,2} The distributions $P(E_T)$ and $\beta(E_T)$ can then be found by a least-squares fit. The weights for the data as a function of E_T and θ in the fitting procedure are calculated from the finite laboratory angular acceptance of the detector.¹³ The angular acceptance has a negligible effect in this case, as shown by the agreement between the $P(E_T)$ and the raw data in Fig. 1. Figure 2 shows fits to the angular distribution at several E_T for the full-power coincident neutral data shown in the middle curve of Fig. 1.

The extracted values of $\beta(E_T)$ for the reduced-power

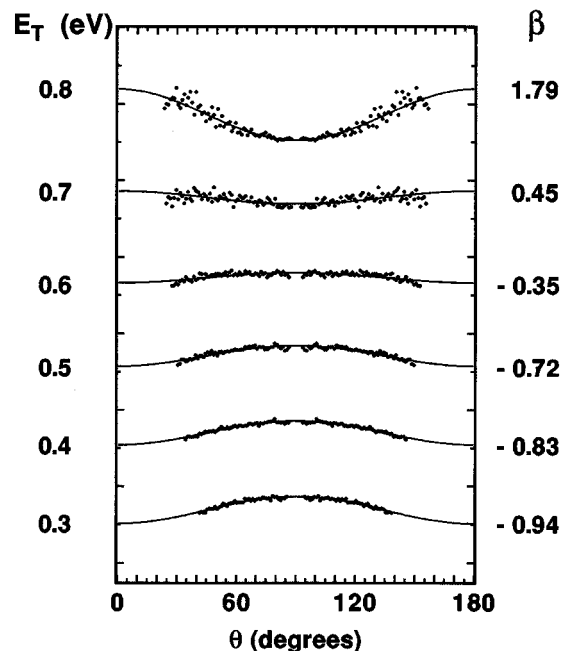


FIG. 2. Center-of-mass angular distributions $I(\theta)$ vs θ at different E_T for coincident neutrals (middle curve of Fig. 1). Points correspond to data and the solid lines show the fits for the anisotropy parameter $\beta(E_T)$. The curves are arbitrarily normalized and symmetrized about $\theta=90^\circ$, since the center-of-mass angle θ is only uniquely defined from 0 to 90° for equal mass photofragments.

coincident neutral data are shown in Fig. 3. This curve shows the large negative value of the anisotropy parameter, $\beta = -0.88 \pm 0.03$, at the peak of the DPD $P(E_T)$. This value is more negative than that recorded at full power ($\beta = -0.83$), probably due to a reduced contribution from ion photodissociation. The values of $\beta(E_T)$ are averaged over 0.1 eV wide energy bins.

Observation of an anisotropic product angular distribution in DPD is a consequence of the alignment produced by photodetachment. In particular, if dissociation of the nascent neutral is rapid and axial recoil occurs, an anisotropic product angular distribution will be observed.^{1,2} The significance of β is different from that in direct photodissociation, however, as the anisotropy is governed by the symmetry of both the initial anion and the final (electron plus neutral) compound state.^{3,5} Thus, even if the initial electronic state is known, the symmetry of the electronic state of the neutral complex is not fixed as there are degenerate continuum states available to the photodetached electron.^{3,5} This assumes that DPD is occurring in the Born–Oppenheimer limit, i.e., that the time scale of electron departure and decay of the neutral are sufficiently different to make an electronic state of the neutral complex a meaningful construct.

The present experiments cannot determine an exact lifetime for the neutral O_4 complex. They do, however, place an upper bound on the complex lifetime. In the case of prompt axial recoil perpendicular to the electric vector of the dissociation laser, the lower limit for β is -1 .^{1,2} As the complex rotates, the anisotropy decreases, reaching an asymptotic value for β of -0.25 in the long-lifetime limit.² The observed $\beta = -0.88$ at the peak of the DPD $P(E_T)$ indicates

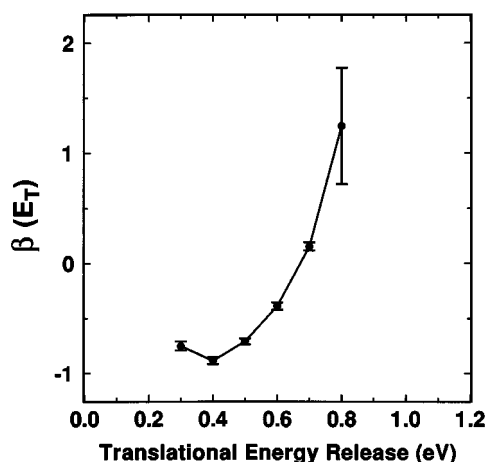


FIG. 3. The energy dependence of the anisotropy parameter, $\beta(E_T)$, for coincident neutrals at reduced laser power. The data points correspond to values for $\beta(E_T)$ averaged over 0.1 eV energy bins. Error bars are $\pm 2\sigma$ as found in a least squares fit to the data.

that dissociation is prompt on the time scale of molecular rotation ($\approx 10^{-12}$ s).

It is interesting to compare the anisotropy observed in the molecular products of DPD with that measured for the photoelectrons at 532 nm by Johnson and co-workers.^{12,17} The photoelectron angular distribution was characterized by an anisotropy parameter of $\beta = -0.9$.¹² This shows that both the photoelectron and the molecular fragments are recoiling in the plane perpendicular to the electric vector of the laser. The photodetachment spectrum of O_4^- they reported shows a broad, featureless distribution peaking at an electron binding energy of 1.6 eV with an energetic threshold at 1 eV. The present result lends credence to the idea that the short lifetime of O_4 may lead to the lack of resolved structure in the photoelectron spectrum.¹⁷

As Fig. 3 shows, $\beta(E_T)$ still rises to large positive values at large E_T , even when the laser power is reduced by a factor of 10. Dynamical effects in DPD may play a role in this energy dependence, however, it is likely that ion photodissociation is responsible for the rise in $\beta(E_T)$. The ion photodissociation signal in the top curve of Fig. 1 is characterized by a large positive β . Ion photodissociation may be detected at low laser power in the neutral coincidence spectra due to residual neutralization of O_2^- by a second photon, as well as rapid (10^{-10} s) vibrational autodetachment of any $O_2^-(v > 3)$ ²⁰ produced in the photodissociation.

Other mechanisms for DPD must also be considered. The peak assigned to DPD may correspond to photodissociation on a repulsive electronic state of different symmetry, followed by rapid autodetachment. There is no evidence for production of $O_2^-(v \leq 3)$ with a large negative β , which makes this seem unlikely. The participation of intermediate autodetaching states of O_4^- in DPD is also possible. Studies of the wavelength dependence of the dynamics will be needed to rule this out.

The $P(E_T)$, peaking at 0.4 eV, can be taken as a measure of the repulsion between the O_2 molecules when suddenly produced at the geometry of the anion. The van der Waals binding energy of $(O_2)_2$ is ≈ 0.07 eV.²¹ If the O_4^- anion had

Franck–Condon overlap with O_4 at the van der Waals minimum, detection of stable O_4 would be possible. No obvious evidence for stable O_4 with microsecond lifetimes was found in the current experiments when the beam was directly monitored with a simple microchannel-plate-based detector lowered into the beam path. Evidence for both repulsive and relatively long-lived excited states (10^{-7} – 10^{-13} s) of O_4 has been found by Helm and co-workers using charge exchange of O_4^+ with various electron-donor targets.²² Charge-exchange neutralization of the cation probes much higher energies than are accessible in our experiments, which are restricted by the electron affinity and photon energy to probing configurations < 1.4 eV above the energy of two separated O_2 molecules. In future experiments, it will be of interest to increase the photon energy and see if these states are accessible by photodetachment.

As more sophisticated calculations of the O_4^- and O_4 potential energy surfaces become available, the present measurements in conjunction with dynamics calculations should provide a critical test of the geometry of the anion relative to the neutral potential energy surface. Franck–Condon excitation from the anion to the neutral should result in a large translational energy release between the O_2 fragments as observed in our experiment. Since the electron has carried away an undetermined kinetic energy, quantitative interpretation of the $P(E_T)$ is of limited value beyond noting that it is consistent with what is known about the stability of O_4^- .^{12,17} The ambiguity due to the electron kinetic energy can be resolved by coincidence experiments in which the energy and angular correlations of the photoelectron and molecular fragments are measured. Such experiments are currently in preparation. These future experiments may also provide a route to the measurement of molecule-fixed photoelectron angular distributions for anions, similar to those discussed theoretically²³ and observed experimentally in the photoionization of dipole-aligned NO ²⁴ and the dissociative photoionization of neutral molecules.²⁵

This experiment marks the first measurement of energy and angular distributions from DPD, and has demonstrated that very anisotropic molecular product angular distributions can be produced. Further investigation of this effect in O_4^- at other photon energies and in other systems will provide new insights into the structure and dynamics of both anions and the transient neutral species produced by photodetachment.

This work was supported in part by the National Science Foundation (CHEM-9321786) and the Donors of the Petroleum Research Fund (ACS-PRF 26520-G6). R.E.C. gratefully acknowledges the Camille and Henry Dreyfus Foundation for a New Faculty Award and the David and Lucile Packard Foundation for a 1994 Fellowship in Science and Engineering.

¹R. N. Zare, *Mol. Photochem.* **4**, 1 (1972).

²R. Bersohn and S. H. Lin, *Adv. Chem. Phys.* **16**, 67 (1969); S.-C. Yang and R. Bersohn, *J. Chem. Phys.* **61**, 4400 (1974).

³J. L. Dehmer and D. Dill, *Phys. Rev. A* **18**, 164 (1978).

⁴R. J. Van Brunt and L. J. Kieffer, *Phys. Rev. A* **2**, 1293 (1970).

⁵R. J. Van Brunt and L. J. Kieffer, *Phys. Rev. A* **2**, 1899 (1970).

⁶C. H. Greene and R. N. Zare, *Annu. Rev. Phys. Chem.* **33**, 119 (1982).

⁷D. M. Neumark, *Accs. Chem. Res.* **26**, 33 (1993).

- ⁸L. C. Lee and G. P. Smith, *J. Chem. Phys.* **70**, 1727 (1979); P. C. Cosby, R. A. Bennett, J. R. Peterson, and J. T. Moseley, *J. Chem. Phys.* **63**, 1612 (1975).
- ⁹K. Hiraoka, *J. Chem. Phys.* **89**, 3190 (1988).
- ¹⁰D. C. Conway, *J. Chem. Phys.* **50**, 3864 (1969).
- ¹¹K. Ohta and K. Morokuma, *J. Phys. Chem.* **91**, 401 (1987).
- ¹²M. J. DeLuca, C. C. Han, and M. A. Johnson, *J. Chem. Phys.* **93**, 268 (1990).
- ¹³R. E. Continetti, D. R. Cyr, D. L. Osborn, D. J. Leahy, and D. M. Neumark, *J. Chem. Phys.* **99**, 2616 (1993).
- ¹⁴M. A. Johnson, M. L. Alexander, and W. C. Lineberger, *Chem. Phys. Lett.* **112**, 285 (1984).
- ¹⁵D. J. Lavrich, M. A. Buntine, D. Serxner, and M. A. Johnson, *J. Chem. Phys.* **99**, 5910 (1993).
- ¹⁶D. P. DeBruijn and J. Los, *Rev. Sci. Instrum.* **53**, 1020 (1982).
- ¹⁷L. A. Posey, M. J. DeLuca, and M. A. Johnson, *Chem. Phys. Lett.* **131**, 170 (1986).
- ¹⁸C.-C. Han and M. A. Johnson, *Chem. Phys. Lett.* **189**, 460 (1992).
- ¹⁹C. R. Sherwood, M. C. Garner, K. A. Hanold, and R. E. Continetti (in preparation).
- ²⁰Y. Hatano, in *Electronic and Atomic Collisions*, edited by D. C. Lorents, W. E. Meyerhof, and J. R. Peterson (Elsevier, New York, 1986), pp. 153–173.
- ²¹C. A. Long and G. E. Ewing, *J. Chem. Phys.* **58**, 4824 (1973).
- ²²H. Helm and C. W. Walter, *J. Chem. Phys.* **98**, 5444 (1993).
- ²³D. Dill, *J. Chem. Phys.* **65**, 1130 (1976).
- ²⁴D. J. Leahy, K. L. Reid, and R. N. Zare, *J. Chem. Phys.* **95**, 1757 (1991).
- ²⁵I. Powis, *Chem. Phys. Lett.* **189**, 473 (1992).